Efficient quantum dot single photon extraction into an optical fiber using a nanophotonic directional coupler

M. Davanço,[1,2,a)] M. T. Rakher,[1] W. Wegscheider,[3] D. Schuh,[3] A. Badolato,[4] and K. Srinivasan[1]

[1]*Center for Nanoscale Science and Technology, National Institute of Standards and Technology, Gaithersburg, Maryland 20899, USA*
[2]*Maryland NanoCenter, University of Maryland, College Park, Maryland 20742, USA*
[3]*Institute for Experimental and Applied Physics, University of Regensburg, Regensburg D-93053, Germany*
[4]*Department of Physics and Astronomy, University of Rochester, Rochester, New York 14627, USA*

(Received 25 May 2011; accepted 6 July 2011; published online 19 September 2011)

We demonstrate a spectrally broadband and efficient technique for collecting emission from a single InAs quantum dot directly into a standard single mode optical fiber. In this approach, an optical fiber taper waveguide is placed in contact with a suspended GaAs nanophotonic waveguide with embedded quantum dots, forming a broadband directional coupler with standard optical fiber input and output. Efficient photoluminescence collection over a wavelength range of tens of nanometers is demonstrated, and a maximum collection efficiency of 6% (corresponding single photon rate of 3.0 MHz) into a single mode optical fiber is estimated for a single quantum dot exciton. © *2011 American Institute of Physics*. [doi:10.1063/1.3617472]

Single epitaxially grown quantum dots (QDs) can serve as bright, stable sources of single photons for applications in quantum information processing.[1] A key limitation of QDs embedded in high refractive index semiconductors is the relatively small fraction of the total QD emission (≈1%)[2,3] that can be collected in free-space by a high numerical aperture optic, a consequence of total internal reflection at the semiconductor-air interface. Embedding the QD in a high quality factor (Q), small mode volume resonator such as a micropillar cavity[4,5] is one approach to improving photon extraction, where ideally one benefits from both a faster radiative rate (Purcell enhancement) and a far-field emission pattern that can be efficiently collected. High extraction efficiencies have indeed been demonstrated with this approach.[6] One challenging aspect of using a high-Q microcavity is the necessity for spectral overlap between a narrow cavity mode and the QD emission line, though tunable geometries[7] can overcome this challenge. Alternatively, spectrally broadband approaches (usually without Purcell enhancement) avoid precise tuning and are needed for efficient spectroscopy of multiple spectrally distinct QD transitions and/or emission from multiple QDs and have recently been pursued using solid immersion lenses[8,9] and in vertically oriented tapered nanowire geometries.[10] Here, we demonstrate a guided wave nanophotonic structure for efficient extraction of PL from a single InAs QD directly into an optical fiber, with an operation bandwidth of tens of nm and an overall single mode fiber collection efficiency of ≈6%. Since collection is directly into an optical fiber, optical losses associated with light extraction using a typical micro-photoluminescence setup and coupling from free-space into an optical fiber are completely avoided. Furthermore, this geometry is planar, avoiding deeply etched, vertically-oriented geometries, and could serve as a platform for waveguide (WG)-based photonic circuits involving single QDs and efficient coupling to optical fibers.

Our structure is a hybrid directional coupler formed by a suspended GaAs channel WG containing InAs QDs and a micron diameter optical fiber taper waveguide (FTW) (Fig. 1(a)). The FTW is an optical fiber whose diameter is adiabatically reduced to a wavelength scale minimum, providing access to an evanescent field for guided wave coupling while maintaining single mode fiber ends and low loss. The GaAs WG (Fig. 1(b)) has a cross-sectional diameter of ≈100 nm, enabling phase matching to the FTW and efficient power transfer between the two WGs.[11] This structure supports single guided modes with strong transverse confinement, into which QD radiation is almost completely coupled. Efficient QD coupling to WG modes phase-matched to the single FTW mode thus leads to efficient extraction of QD emission into the fiber. Detailed simulations have predicted a single QD fluorescence collection efficiency as high as ≈ 35% into

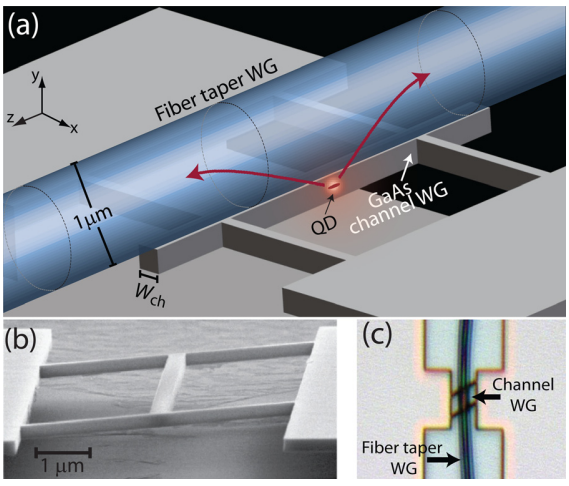

FIG. 1. (Color online) (a) Nanophotonic directional coupler for single photon extraction from a single embedded QD. (b) SEM image of a fabricated GaAs channel WG. (c) Optical microscope image of the FTW/channel WG directional coupler.

[a)]Electronic mail: mdavanco@nist.gov.

an optical fiber (≈ 70% including both fiber ends), with an operation bandwidth of tens of nm.[11]

We first assessed the directional coupler without QDs, to confirm the basic light transfer mechanism between FTW and channel WG. A first set of suspended WGs with no QDs was fabricated on a 250 nm thick GaAs wafer for passive directional coupler characterization.[12] An ≈1 μm diameter FTW was brought into contact with individual channel WGs, forming directional couplers as illustrated in Fig. 1(c). Transmission spectra were obtained by launching broadband polarized light from a tungsten halogen lamp into the FTW input and analyzing output light with an optical spectrum analyzer. The FTW and channel WG each support a single guided mode of TE-like (x-oriented electric field) and TM-like (y-oriented electric field) polarizations. The resulting directional coupler supports a pair of hybrid supermodes for each polarization (Fig. 2(a)).[11] The transmission spectrum for a given polarization is determined by the beating of the corresponding coupler supermodes and exhibits minima when power is transferred from the FTW to the channel WG but not back into the FTW due to termination of the channel.[12]

Several 8 μm long WGs with widths between 240 nm and 340 nm were measured. The transmission spectra (Fig. 2(b)) for the two main coupler polarizations displayed broad, >40 nm wide minima which typically reached >90% extinction, evidencing efficient power transfer between the FTW and suspended WGs. After optical characterization, WG widths were measured with a scanning electron microscope. Figure 2(c) shows minimum transmission wavelengths as a function of WG width, along with the phase-matching wavelengths calculated with a vector finite element method.[11] The minima closely follow the calculated phase-matching wavelengths. The higher rate with which the TE-like phase-matching wavelength shifts with WG width is expected from these modes' higher intensity at the WG sidewalls. The agreement between theoretical and experimental curves indicates that the expected efficient directional coupler operation is indeed achieved.

We next attempted to validate efficient PL extraction from a second set of devices fabricated on a high QD density portion of the same wafer, where the QD ensemble s-shell emission peak was at ≈1200 nm. The QD-containing WGs were probed with a ≈1 μm diameter FTW in a cryostat at <9 K temperature with the setup shown in Fig. S-3 of the supporting materials.[12] The devices were excited by launching a 50 MHz repetition rate, 50 ps width, 780 nm laser pulse train into the FTW. Figures 2(d)–2(f) show TE polarization transmission and corresponding PL spectra for three devices of varying WG widths. PL collection over a range of a few tens of nm is achieved in all cases. The collected PL is maximized when the transmission dip—and thus the phase-matching wavelength—is aligned with the s-shell PL peak, evidencing efficient power transfer between phase-matched WGs. Fiber-collected PL of individual emission lines was typically 10 to 100 times higher than that obtained via free-space collection (from the same devices) with a 0.42 numerical aperture objective. Estimating the absolute collection efficiency was difficult, however, as the high density of QD lines prevented accurate determination of the intensity of any individual transition.

To avoid this difficulty, a third set of devices was fabricated with a low density of QDs, so that well-isolated transitions could be observed. These devices were produced from a 190 nm thick, GaAs WG layer wafer containing QDs with ensemble s-shell emission near 940 nm. Low-temperature PL spectroscopy was performed as above, with a 50 MHz pulsed pump at 780 nm. Figure 3(a) shows the PL spectrum from the device that yielded the highest collection efficiency, for the sharp excitonic line at 957.7 nm. Driving this transition towards saturation (inset, Fig. 3(a)), at 550 nW pump power, we estimate a collection efficiency into a single mode optical fiber $\eta = 6.05\% \pm 0.061\%$.[12] We point out that the transmission of the collection portion of the FTW is ≈84%, so collection into the FTW (our first collection optic) is $7.250\% \pm 0.072\%$. The most likely reason for smaller collection efficiencies than predicted is non-optimal positioning of the QD in the GaAs WG, as supported by simulations presented in the supplementary material.[12]

The 957.7 nm, transition was located outside the operating wavelength band of the tunable bandpass filter available for spectral isolation, preventing further characterization of this device. A second WG was available, however, that

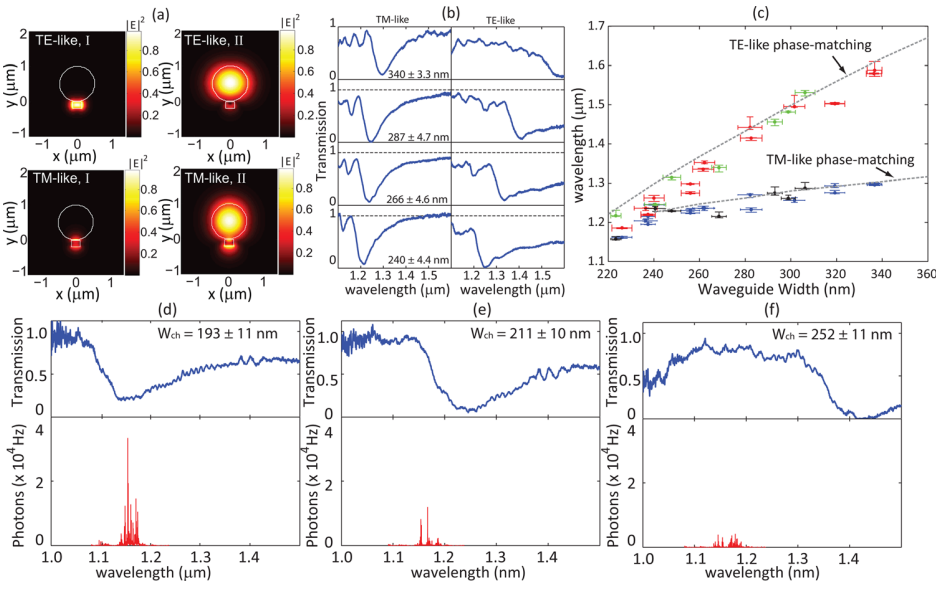

FIG. 2. (Color online) (a) Electric field amplitude squared for the TE-like (top) and TM-like (bottom) supermode pairs of the directional coupler. (b) TE-like and TM-like transmission spectra for suspended channel WGs of varying widths, probed with a ≈1 μm FTW at room temperature. (c) Evolution of transmission minima with WG widths for the two polarizations in (a). Dashed lines are calculated phase-matching wavelengths for the fiber and WG. (d)-(f): Low temperature (≈8 K) transmission and corresponding fiber-collected PL for WGs with increasing widths W_{ch}.

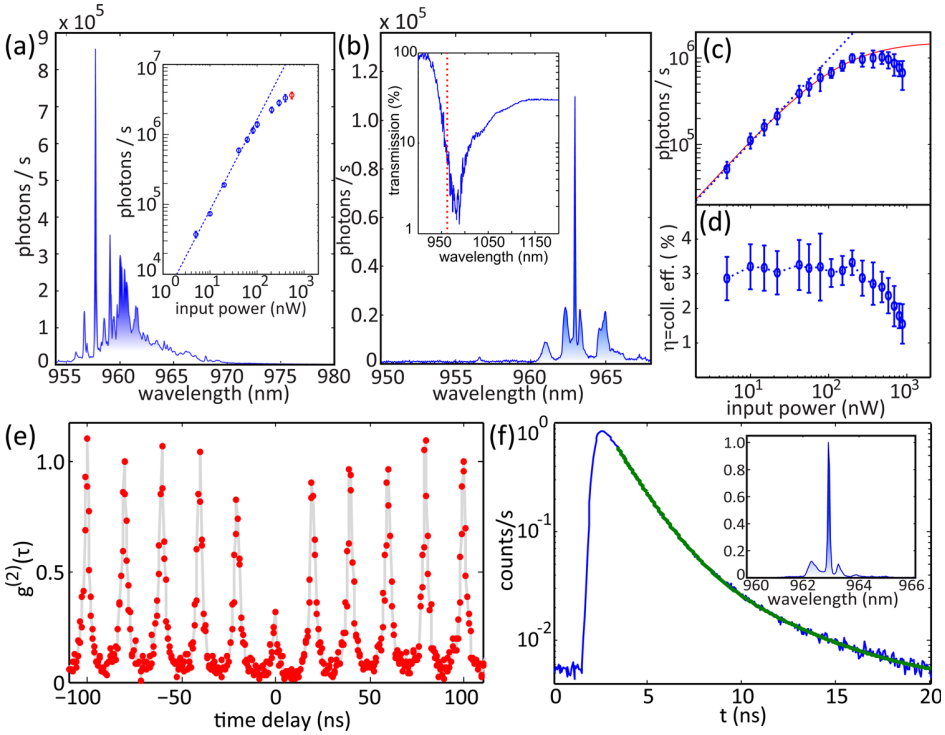

FIG. 3. (Color online) (a) Fiber-collected single QD PL for the brightest device. Inset: photon rate for 957.7 nm line against pump power. (b) Fiber-collected single QD PL for second WG. Inset: directional coupler transmission spectrum, showing position of QD line. (c) Collected PL rate versus excitation power for 963 nm line in (b). Error bars are 95% fit confidence intervals. Dashed line: linear fit to data below saturation. Continuous line: fit to theory. (d) Fiber collection efficiency obtained from (c), assuming ideal QD behavior. (e) Second-order correlation $g^{(2)}(\tau)$ and (f) lifetime for the excitonic line in (b), after a 1 nm bandpass filter (inset spectrum). Green line: bi-exponential fit.

displayed an isolated transition at ≈963 nm, shown in Fig. 3(b), located within the coupler transmission dip (inset). The evolution of the 963 nm peak collected PL rate into the single mode fiber as a function of pump power is shown in Fig. 3(c). For $P_{in} < 100$ nW, integrated PL counts increase linearly with pump power. A fit to the data assuming an ideal single exciton QD line (Fig. 3(c))[12] matches the data for $P_{in} < 100$ nW, but overestimates the PL rate for $P_{in} > 100$ nW. For the highest measured PL intensity, the integrated counts correspond to $\eta \approx 2\%$. For $P_{in} \ll P_{sat} \approx 133$nW, where the QD can be assumed to behave ideally, however, $\eta \approx 3\%$ (Fig. 3(d)).

To confirm the single photon nature of the 963 nm line of Fig. 3(b), we measured the second-order correlation, $g^{(2)}(\tau)$, for pulsed excitation at $P_{in} \approx 75$ nW (Fig. 3(e)). $g^{(2)}(0) = 0.29 \pm 0.02$,[12] indicating single QD emission that is dominantly comprised of single photons. The nonzero $g^{(2)}(0)$ is likely due to insufficient filtering, which allows uncorrelated photons and possible emission from other QDs to be detected. In particular, the spectrum of the detected light (inset in Fig. 3(f)) contains two broad sidelobes in addition to the 963 nm excitonic line. These may correspond to emission from other QDs with broadened lines, owing to proximity to WG sidewalls.[13] A bi-exponential decay of the excitonic line (Fig. 3(f)) with fast and slow lifetimes of 1.48 ns ± 0.08 ns and 4.6 ns ± 0.8 ns (uncertainties are 95% fit confidence intervals) evidences non-ideal QD behavior. This is consistent with what is seen in $g^{(2)}(\tau)$ (Fig. 3(e)), where the coincidence counts between peaks do not return all the way to zero. The fast decay constant approaches the lifetime of a typical InAs QD (the lack of radiative rate enhancement is predicted in simulations),[11] while the long decay evidences QD coupling to nonradiative states that may lead to a reduced quantum efficiency and collection efficiency estimates.

In summary, we have demonstrated a fiber-coupled, QD single photon source based on a planar, guided wave nanophotonic coupler. We use this spectrally broadband approach to demonstrate an in-fiber, single QD PL collection efficiency of 6%. Future work is aimed at improved efficiency through precise QD location[14,15] within the device and understanding sources of non-ideal QD behavior.

This work was partly supported by the NIST-CNST/UMD-NanoCenter Cooperative Agreement. We thank R. Hoyt, C. S. Hellberg, Alexandre M. P. A. Silva, and Hugo Hernández-Figueroa for useful discussions.

[1]A. J. Shields, Nature Photon. **1**, 215 (2007).
[2]H. Benisty, H. D. Neve, and C. Weisbuch, IEEE J. Quantum Electron. **34**, 1612 (1998).
[3]W. L. Barnes, G. Björk, J. Gérard, P. Jonsson, J. A. E. Wasey, P. T. Worthing, and V. Zwiller, Eur. Phys. J. D **18**, 197 (2002).
[4]G. Solomon, M. Pelton, and Y. Yamamoto, Phys. Rev. Lett. **86**, 3903 (2001).
[5]M. Pelton, C. Santori, J. Vuckovic, B. Zhang, G. S. Solomon, J. Plant, and Y. Yamamoto, Phys. Rev. Lett. **89**, 233602 (2002).
[6]S. Strauf, N. G. Stoltz, M. T. Rakher, L. A. Coldren, P. M. Petroff, and D. Bouwmeester, Nature Photon. **1**, 704 (2007).
[7]A. Muller, E. B. Flagg, M. Metcalfe, J. Lawall, and G. S. Solomon, Appl. Phys. Lett. **95**, 173101 (2009).
[8]V. Zwiller and G. Bjork, J. Appl. Phys. **92**, 660 (2002).
[9]A. N. Vamivakas, M. Atatüre, J. Dreiser, S. T. Yilmaz, A. Badolato, A. K. Swan, B. B. Goldberg, A. Imamoğlu, and M. S. Ünlü, Nano Lett. **7**, 2892 (2007).
[10]J. Claudon, J. Bleuse, N. S. Malik, M. Bazin, P. Jaffrennou, N. Gregersen, C. Sauvan, P. Lalanne, and J. Gérard, Nature Photon. **4**, 174 (2010).
[11]M. Davanço and K. Srinivasan, Opt. Lett. **34**, 2542 (2009).
[12]See supplementary material at http://dx.doi.org/10.1063/1.3617472 for additional experimental, simulation, and nanofabrication details.
[13]C. F. Wang, A. Badolato, I. Wilson-Rae, P. M. Petroff, E. Hu, J. Urayama, and A. Imamoglu, Appl. Phys. Lett. **85**, 3423 (2004).
[14]K. Hennessy, A. Badolato, M. Winger, D. Gerace, M. Atature, S. Guide, S. Falt, E. Hu, and A. Imamoglu, Nature (London) **445**, 896 (2007).
[15]S. M. Thon, M. T. Rakher, H. Kim, J. Gudat, W. T. M. Irvine, P. M. Petroff, and D. Bouwmeester, Appl. Phys. Lett. **94**, 111115 (2009).